Proceedings of the 2004 IEEE
International Conference on Robotics & Automation
New Orleans, LA • April 2004

Hopping Direction Controllability for Small Body Exploration Robot

Shingo Shimoda
The University of Tokyo, Japan
Email: shimoda@nnl.isas.ac.jp

Andreas Wingert
The University of Tokyo, Japan
Email: arw@nnl.isas.ac.jp

Kei Takahashi
The University of Tokyo, Japan
Email: kei@nnl.isas.ac.jp

Takashi Kubota
ISAS/JAXA, Kanagawa, Japan
Email: kubota@nnl.isas.ac.jp

Ichiro Nakatani
ISAS/JAXA, Kanagawa, Japan
Email: nakatani@nnl.isas.ac.jp

Abstract— **Hopping is effective mobility for exploration robot on small body. To explore small bodies, a mobile robot is required to move to target points. In case of exploration of microgravity environment by a hopping locomotion, hopping trajectories cannot be controlled after a robot hops. To move to target points, hopping direction and velocity should be controlled at takeoff. The authors proposed a hopping robot, which consists of three masses, two linear actuators and a spring. This paper discusses how to control a hopping direction of the proposed robot in microgravity environment. When the robot hops, the friction force between the robot and the ground becomes larger. The simulation results show the controllability of a hopping direction even if there is a slip on a ground. The controllability is also confirmed by the free fall experiments.**

I. Introduction

Mobile robots require high mobility systems in planetary exploration because mobile robots should move to targets, pick up desired samples and set instruments at any point. Therefore, various kinds of robots and systems have been proposed and developed to move in various environments[1][2][3][4][5][6].

Especially, in case of mobile robots for small bodies, such as asteroids and comets, special locomotion mechanisms are required due to their weak gravity. The friction forces between robots and grounds are so small that conventional wheel robots and legged robots cannot obtain enough horizontal velocities to observe large areas.

Hopping is one of the effective mobility to move in the microgravity environment[7][8][9][10][11]. To hop in microgravity environment, a hopping robot should push grounds. By pushing ground, normal force between a robot and a ground becomes larger. When normal force becomes larger, friction force between a robot and a ground also becomes larger. A hopping robot can obtain horizontal velocity using the friction force.

To move to target points by hopping mobility, two abilities are required. One ability is the precise hopping control. A moving trajectory of a hopping robot is determined at takeoff. Once a hopping robot is airborne, it cannot alter its trajectory. To accurately approach the target point, the velocity and direction of hopping need to be controlled, which is a function of hop mechanisms and interactions between a robot and ground.

The other ability is a landing on the surface exactly. A hopping robot might bounce, slip and tip over if there is no landing function. This means that a robot cannot reach targets even if the robot hops with correct velocity and direction. Therefore, hopping robots should control both hopping and landing.

The asteroid exploration spacecraft "HAYABUSA" (MUSES-C)[12] launched in May, 2003 carries the small exploration robot "MINERVA"[8], which has the hopping mobility. MINERVA, however, does not move to the desired point exactly, because it does not any landing mechanism.

The authors have proposed a hopping mechanism that is composed with three masses, two linear actuators and a spring[13][14]. The proposed mechanism can be used for hopping and landing. The landing mechanism was discussed in [14]. This paper describes a control method to hop in the desired direction. The horizontal velocity is obtained using the friction force. To generate the large friction force, the large pressure is required. However, the large pressure generates the large horizontal velocity. These facts might show a limitation of the hopping angle. The controllability of the hopping direction is discussed by the simulation studies and the free fall experiments in this paper.

This paper is organized as follows. In section 2, the structure of the proposed robot is described, and the theoretical limitation of the hopping angle is considered. In section 3, the controllability of the hopping angle is discussed by the simulation studies. Especially the cases with slip and without slip on the ground are compared, and the controllability of the hopping angle with slip is described. In section 4, the controllability of the hopping angle is confirmed by the free fall experiments. In section 5, the conclusion of this paper is summarized.

II. Mobility of Proposed Robot

A. Structure

The model of the proposed robot is described in Fig.1. M_1 and M_2 are connected by the spring and the ultrasonic linear

0-7803-8232-3/04/$17.00 ©2004 IEEE

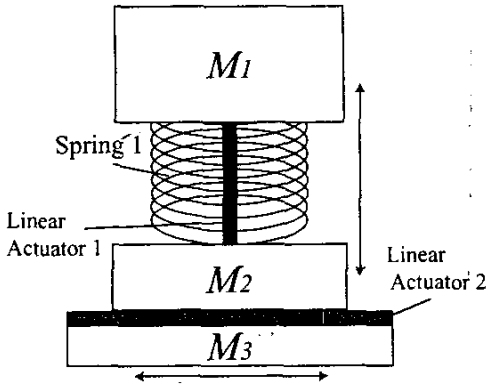

Fig. 1. Model of Spring Mechanism

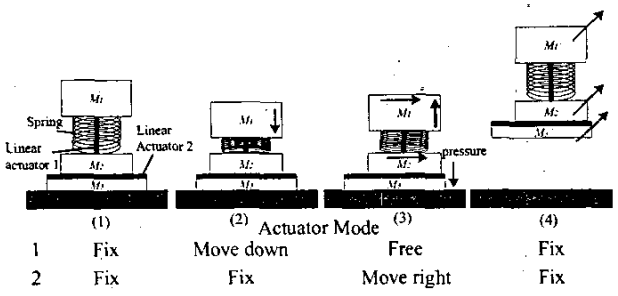

Fig. 2. Actuator Mode and Movement of Robot at Hopping

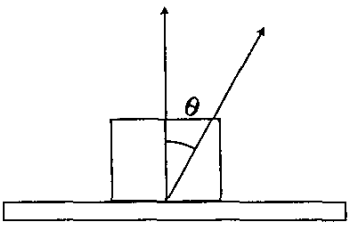

Fig. 3. Definition of Hop Angle θ

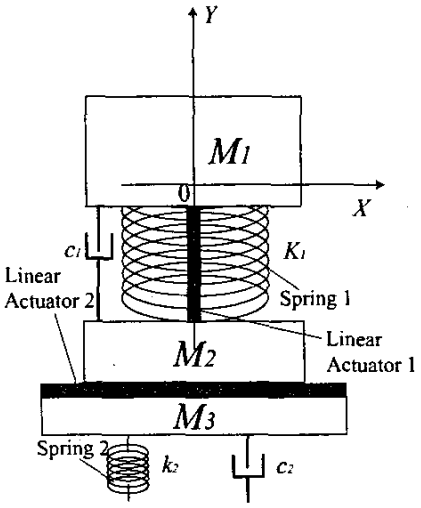

Fig. 4. Coordinate System and Simulation Model

actuator. The linear actuator can be driven with three states, the fixed mode, the drive mode and the free mode. The length of the spring is fixed when the linear actuator is driven with the fixed mode. The spring is compressed when the linear actuator is driven with the drive mode. The M_1 and M_2 can move freely by the spring force when the linear actuator is driven with the free mode.

M_2 and M_3 are connected by another linear actuator. The linear actuator can drive M_2 in the horizontal direction relative to M_3. M_1 moves with the same velocity of M_2 in the horizontal direction.

B. Hopping Direction

The proposed robot can hop with the horizontal velocity by transforming the elastic energy to the kinetic energy as shown in Fig.2. From the stationary state, M_1 is pulled down by the linear actuator(Fig.2 (2)). At this state, the spring is compressed, so the elastic energy is charged inside the robot. By changing the actuator mode to the free mode, M_1 is pushed in the upward and the velocity in upward is obtained. At this state, M_2 is pushed in the downward (Fig.2 (3)). When M_2 is pushed into the downward, M_3 is pressed to the ground. The normal force between M_3 and the ground becomes larger by the pressure. When the linear actuator between M_2 and M_3 is driven, M_2 and M_1 move and obtain the momentum of the horizontal direction. However M_3 does not move if the driving force is smaller force than the friction force between M_3 and the ground. When the length of the spring becomes normal, M_1 has the momentum of the vertical and the horizontal directions, M_2 has the momentum of the horizontal direction and M_3 has no momentum. Therefore, the robot can hop with the horizontal velocity.

When the pressure between M_3 and the ground is represented by F_p, the limitation of the friction force is expressed as follows[15]:

$$F_f = \mu F_p \tag{1}$$

F_f : Limitation of Friction Force
μ : Friction Coefficient

The limitation of the hopping angle θ is expressed as follows(Fig.3):

$$\theta < \arctan \frac{F_f}{F_p} = \arctan \mu \tag{2}$$

This equation shows that the hopping direction is controllable in the limitation that depends on the friction coefficient.

III. Simulation Study

A. Condition of Simulation

To investigate the controllability of the hopping direction, computer simulations are performed on the following conditions:

1) The coordinate system is shown in Fig.4. The origin is set on the center of gravity of the robot.
2) There is no relative motion between M_1 and M_2 in the x-direction by constraint of the linear actuator. Therefore, M_1 and M_2 are lumped into a single mass in x-direction simulation. Similarly, for the motion in the y-direction masses M_2 and M_3 are considered a single mass.
3) The contact model is described by a spring and damper model.
4) Each parameter is set as follows:
   M_1=2.2[kg], M_2=0.8[kg], M_3=0.2[kg], k_1=100[N/m], c_1=10[Ns/m], k_2=10000[kg], c_2=100[Ns/m]

B. Equation of Motion

The equation of motion is shown as follows.

$$\boldsymbol{X} = \begin{bmatrix} x_1 & \dot{x}_1 & x_3 & \dot{x}_3 & y_1 & \dot{y}_1 & y_2 & \dot{y}_2 \end{bmatrix}^T \tag{3}$$

$$\dot{\boldsymbol{X}} = \begin{bmatrix} 0 & 1 & 0 & 0 \\ 0 & 0 & 0 & 0 \\ 0 & 0 & 0 & 1 \\ 0 & 0 & 0 & 0 \\ 0 & 0 & 0 & 0 \\ 0 & 0 & 0 & 0 \\ 0 & 0 & 0 & 0 \\ 0 & 0 & 0 & 0 \end{bmatrix} \begin{bmatrix} 0 & 0 & 0 & 0 \\ 0 & 0 & 0 & 0 \\ 0 & 0 & 0 & 0 \\ 0 & 0 & \frac{\mu k_2}{m_3} & 0 \\ 0 & 1 & 0 & 0 \\ -\frac{k_1}{m_1} & -\frac{c_1}{m_1} & \frac{k_1}{m_1} & \frac{c_1}{m_1} \\ 0 & 0 & 0 & 1 \\ \frac{k_1}{m_2+m_3} & \frac{c_1}{m_2+m_3} & -\frac{k_2+k_1}{m_2+m_3} & -\frac{c_2+c_1}{m_2+m_3} \end{bmatrix} \boldsymbol{X} + \begin{bmatrix} 0 \\ \frac{F_x}{m_1+m_2} \\ 0 \\ -\frac{F_x}{m_3} \\ 0 \\ \frac{F_y}{m_1} \\ 0 \\ -\frac{F_y}{m_2+m_3} \end{bmatrix} \tag{4}$$

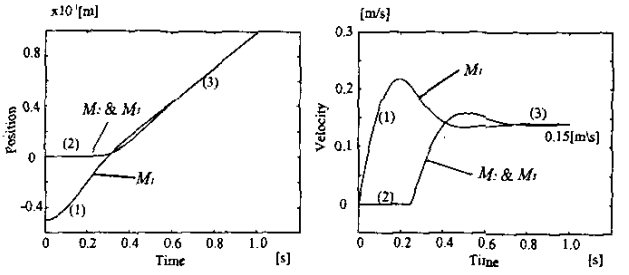

Fig. 5. Hopping Simulation Result in Vertical Direction: The time history of the position and velocity of each mass in y-direction

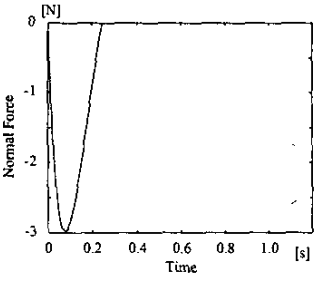

Fig. 6. Hopping Simulation Result: The time history of the normal force between M_3 and the ground

x_1 : Position of M_1 and M_2 in x − direction
x_3 : Position of M_3 x − direction
y_1 : Position of M_1 iny − direction
y_2 : Position of M_2 and M_3 in y − direction
m_* : Mass of M_*
k_1 : Spring Coefficient
c_1 : Damping Coefficient
k_2 : Spring Coefficient of Contact Model
c_2 : Damping Coefficient of Contact Model
F_y : Force of Linear Actuator 1
F_x : Force of Linear Actuator 2
μ : FrictionCoefficient

C. Simulation Result in Vertical Direction

At the hopping simulation, the initial values are set as follows:

$$\boldsymbol{X}_0 = \begin{bmatrix} 0 & 0 & 0 & 0 & -5.0 \times 10^{-2} & 0 & 0 & 0 \end{bmatrix}^T \tag{5}$$

This state means that the spring 1 is compressed in 5.0×10^{-2}[m].

The simulation results in vertical direction are shown in Fig.5 and Fig.6. At the time 0, the mode of the linear actuator 1 is changed to the free mode. At this state, the spring force works to M_1 in the upward. M_1 can move freely in the upper direction so that M_1 obtains the velocity in vertical direction(Fig.5 (1)). On the other hand, the spring force also

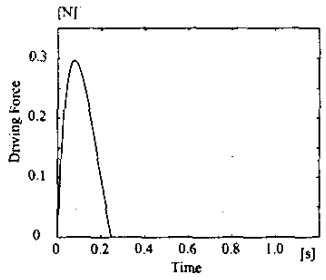

Fig. 7. Hopping Simulation Result: The time history of the driving force when the linear actuator 2 is driven without slipping on the ground

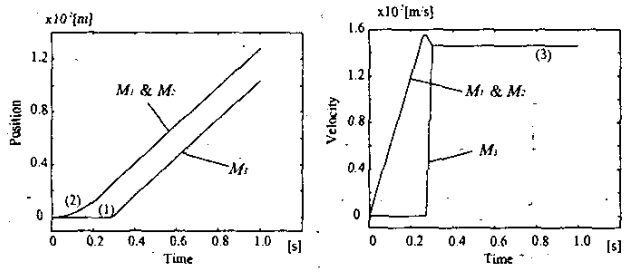

Fig. 8. Hopping Simulation Result in Horizontal Direction: The time history of the position and the velocity without slipping

works to M_2 and M_3 in the downward. At this state, M_3 cannot move to downward because M_3 contacts with the ground(Fig.5 (1)). So M_3 is pressed to the ground by the spring force. The pressure to the ground is described in Fig.6.

0.3[s] later, the pressure becomes 0. All masses hop with the velocity 1.5×10^{-1}[m/s] by fixing the linear actuator 1(Fig.5 (3)).

D. Simulation Result in Horizontal Direction

As shown in Fig.6, there is the pressure between M_3 and the ground when the robot hops. Using the pressure, the robot can obtain the horizontal velocity.

Here suppose that the friction coefficient $\mu = 0.1$. To obtain the horizontal velocity without slipping on the ground, the actuator 2 is driven as shown in Fig.7. In this case, the time history of the position and the velocity of each mass are described in Fig.8. As shown in Fig.8 (1), M_3 does not move until the pressure becomes 0. However, M_1 and M_2 can obtain the horizontal velocity(Fig.8 (2)). After the pressure become 0, the horizontal velocity of the robot becomes 1.5×10^{-2}[m/s](Fig.8 (3)).

To control the linear actuator without slipping, the pressure or the slip should be measured. However, the time that the pressure works is approximately 0.3[s]. It is very difficult to measure the pressure or the slip and feedback to the controller of the actuator 2. Therefore, the next simulations show the results that the linear actuator 2 is driven with the constant forces.

In case of the linear actuator 2 force $F_X = 0.1$[N], the time

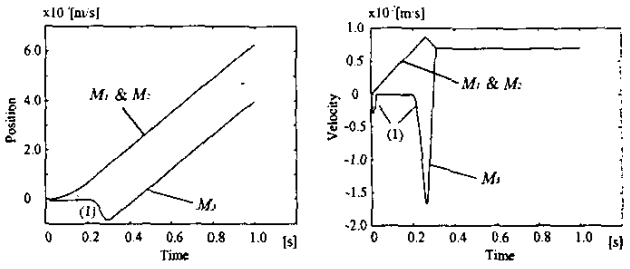

Fig. 9. Hopping Simulation Result in Horizontal Direction: The time history of the position and the velocity when the driving force is 0.1[N]

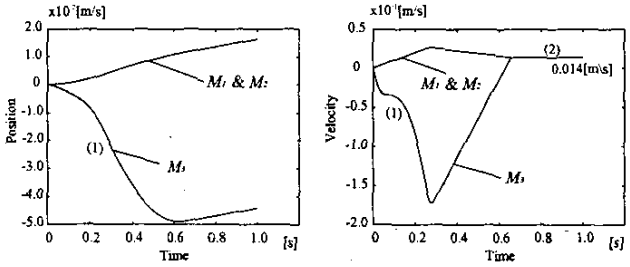

Fig. 10. Hopping Simulation Result in Horizontal Direction: The time history of the position and the velocity when the driving force is 0.3[N]

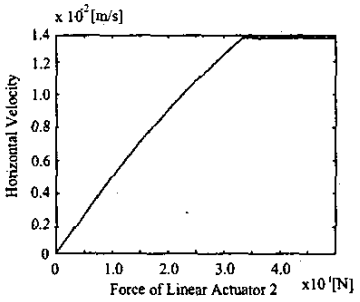

Fig. 11. Hopping Simulation Result: Driving Force vs. Horizontal Velocity

history of the position and the velocity of each mass is shown in Fig.9. From the result, the slip of M_3 on the ground can be observed(Fig.9 (1)). The horizontal velocity of the robot is 0.5×10^{-2}[m/s]. The horizontal velocity of the result is smaller than the result without slip.

When the linear actuator 2 is driven with $F_X = 0.3$[N], the result of the simulation is shown in Fig.10. The slip of M_3 was also observed(Fig.10 (1)). However, the horizontal velocity of the robot is 1.4×10^{-2}[m/s](Fig.10 (2)). The horizontal velocity is approximately the same as the result without slipping. It can be explained that M_3 is so light comparing with M_1 and M_2 that the influence of the momentum of M_3 is small.

The relationship between the force of the actuator 2 and the horizontal velocity is described in Fig.11. This result shows that the horizontal velocity can be controlled by the constant force of the linear actuator 2 and the maximum horizontal

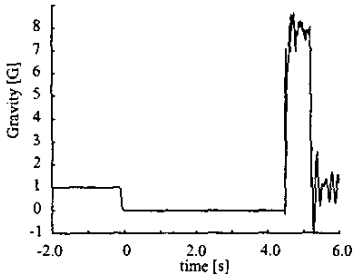

Fig. 12. Time History of Gravitational Acceleration in Free Fall Experiment

TABLE I
PARAMETERS AND RESULT IN FREE FALL EXPERIMENTS

	μ	F_x [N]	v_y [m/s]	v_x [m/s]	Slip
1	1.0	2.0	9.0×10^{-2}	1.8	X
2	1.0	3.0	9.0×10^{-2}	3.0	X
3	0.1	2.0	9.0×10^{-2}	1.7	X
4	0.1	3.0	9.0×10^{-2}	2.0	O

velocity is not so different comparing with the non-slipping hop.

IV. Free Fall Experiment

A. Experimental Condition

To confirm the hopping ability of the proposed robot, the free fall experiments were conducted. In free fall experiments, the experimental setup is set in the capsule. The capsule falls freely in the drop shaft, thereby providing a microgravity environment inside the capsule for about 4.5[s]. The time history of the gravitational acceleration is shown in Fig.12.

B. Prototype of Robot

The prototype hopping robot was developed as shown in Fig.13. The developed robot is composed with three masses, two linear actuators and a spring. The each parameter is shown as follows:
M_1=2.2[kg], M_2=0.8[kg], M_3=0.2[kg], k_1=100[N/m]

C. Experimental Results

The independent parameters in the experiments are the driving force of the linear actuator 2 and the friction coefficient. The motion of the robot is recorded on video as sequential image data. The overview of the experiment is shown in Fig.14 and the test parameters and results are summarized in Table.I.

The vertical velocity was controlled to 9.0×10^{-2}[m/s] in all the experiments. In case that the friction coefficient is 1.0, the hopping angle increases with increasing the force of the linear actuator 2. The slips were not observed.

On the other hand, in case of $\mu = 0.1$, the horizontal velocities were smaller than the case of $\mu = 1.0$. Especially in case that the linear actuator 2 was driven with 3[N], the slip of M_3 on the ground was observed.

From the results, the following things can be obtained:

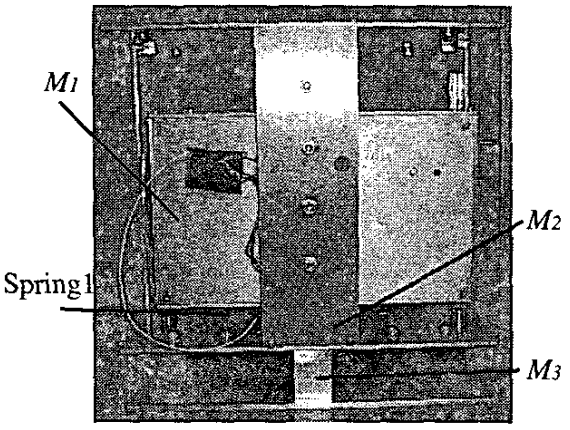

Fig. 13. Overview of Prototype Robot

- The robot can obtain the horizontal velocity even if there is a slip on the ground.
- The horizontal velocity can be controlled by the constant force of the linear actuator 2. The results show that the hopping direction can be controlled.
- The horizontal velocity becomes small when M_3 slips on the ground. This means that the maximum hop angle depends on the friction coefficient.

V. Conclusion

The conclusion of this paper is summarized as follows:

1) The hopping mechanism that can be used for hopping and landing is described. The robot with the proposed mechanism can hop with horizontal velocity. However, there is the limitation of the hopping angle. The limitation angle θ is theoretically expressed by the equation of $\theta = \arctan\mu$. μ is the friction coefficient between the robot and the ground.
2) The controllability of the hopping direction is shown by the simulation studies. It is also shown that there is a limitation of the hopping angle. The limitation of the hopping angle does not change even if there is a slip between the robot and ground. The limitation of the hopping angle in the simulation is 1.3×10^{-1}[rad] in case of $\mu = 0.1$.
3) The controllability of the hopping direction and the limitation of the hopping angle were confirmed by the free fall experiments.

Fig. 14. , Overview of Hopping Experiment

ACKNOWLEDGEMENT

This work was partially supported by "Ground Research Announcement for Space Utilization" promoted by Japan Space Forum.

REFERENCES

[1] A. Mishkin, J. Morrison, T. Nguyen, H. Stone, B. Cooper, and B. Wilcox, "Experiences with Operations and Autonomy of the Mars Pathfinder Microrover," *Proc. of IEEE Aerospace Conf.*, 1998.

[2] J. Matijevic, "Characterization of Martian Surface Deposite by the Mars Pathfinder Rover, Sojourner," *Science*, , no. 278, pp. 237–242, 1997.

[3] S.Hayati and R.Arvidson, "Long Range Science Rover (Rocky 7) Mojave Deset Field Tests," *Proceedings of International Symposium on Artificial Intelligence, Robotics and Automation in Space*, pp. 361–370, 1997.

[4] K.Iagnemma, F.Genot, and S.Dubowsky, "Rapid Physics-Based Rough-Terrain Rover Planning with Sensor and Control Uncertainty," *Proceedings of the 1999 IEEE International Conference on Robotics and Automation*, pp. 2286–2291, 1999.

[5] S.Moorehead, R.Simmons, D.Apostolopoulos, and W.Whittaker, "AUTONOMOUS NAVIGATION FIELD RESULTS OF A PLANETARY ANALOG ROBOT IN ANTARCTICA," *Proc. Fifth International Symposium on Artificial Intelligence, Robotics and Automation in Space*, pp. 237–242, 1999.

[6] K.Watanabe, S.Shimoda, T.Kubota, and I.Nakatani, "A Mole-Type Drilling Robot for Lunar Subsurface Exploration," *The 7th International Symposium on Artificial Intelligence, Robotics and Automation in Space*, 2003.

[7] T. Kubota, B. Wilcox, H. Saito, J. Kawaguchi, R. Jones, A. Fujiwara, and J.Reverke, "A Collaborative Micro-Rover Exploration Plan on the Asteroid Nereus in MUSES-C Mission," *48th International Astronautical Congress*, 1997.

[8] T.Yoshimitsu, T.Kubota, S.Akabane, I.Nakatani, T.Adachi, H.Saito, and Y.Kunii, "Autonomous Navigation and Observation on Asteroid Surface by Hopping Rover MINERVA," *The 6th International Symposium on Artificial Intelligence, Robotics and Automation in Space: A New Space Odyssey, AS017*, 2001.

[9] Y.Nakamura, S.Shimoda, and S.Shoji, "Mobility of a Microgravity Rover Using Internal Electro-Magnetic Levitation," *Proceedings of the 2000 IEEE/RSJ International Conference on Intelligent Robots and Sytems*, pp. 1639–1645, 2000.

[10] J.Burdick and B.Goodwine, "Quasi-Static Legged Locomotors as Nonholonomic System," *Proceedings of the 2000 IEEE/RSJ International Conference on Intelligent Robots and Sytems*, pp. 867–872, 2000.

[11] K.Yoshida, "The Jumping Tortoise: A Robot Design for Locomotion on Micro Gravity Surface," *Proceedings of The 5th International Symposium on Artificial Intelligence, Robotics and Automation in Space*, pp. 705–707, 1999.

[12] "http://www.isas.ac.jp/e/enterp/missions/muses-c/index.shtml," .

[13] S.Shimoda, T.Kubota, and I.Nakatani, "New Mbility System Based on Elastic Energy under Microgravity," *Proceedings of the 2002 IEEE International Conference on Robotics and Automation*.

[14] S.Shimoda, A.Wingert, K.Takahashi, T.Kubota, and I.Nakatani, "Microgravity Hopping Robot with Controlled Hopping and Landing Capability," *Proceedings of the 2003 IEEE/RSJ International Conference on Intelligent Robots and Sytems*, 2003.

[15] T.Yoshimitsu, T.Kubota, and I.Nakatani, "New Mobility System for Small Planetary Body Exploration," *Proceedings of the 1998 IEEE International Conference on Robotics and Automation*, 1999.